Orientationally disordered H_2 in the high-pressure van der Waals compound $SiH_4(H_2)_2$

Yinwei Li, Guoying Gao, Quan Li, Yanming Ma,* and Guangtian Zou
State Key Laboratory of Superhard Materials, Jilin University, Changchun 130012, China
(Received 22 July 2010; published 16 August 2010)

Recent high-pressure synthesis of H_2-rich van der Waals compounds have attracted great interests in probing novel H_2 physics, which in general remain elusive. We have solved the crystal structure of the synthesized $SiH_4(H_2)_2$ by first-principles calculations and revealed that SiH_4 molecules in the formation of $SiH_4(H_2)_2$ remain nearly unaltered with Si atoms forming a peculiar tetragonal lattice, which can also be viewed as a distorted face-centered-cubic lattice. We have provided direct evidences on that H_2 molecules in $SiH_4(H_2)_2$ occupy the interstitial sites, and more intriguingly are orientationally disordered. Our argument has been supported by the excellent mutual agreement between theoretical and experimental equation of states, Raman, and x-ray diffraction data. The current study has strong implications on other high-pressure van der Waals compounds, e.g., H_2O-H_2, CH_4-H_2, NH_3BH_3-H_2, Ar-H_2, and Xe-H_2.

DOI: 10.1103/PhysRevB.82.064104 PACS number(s): 61.50.Ah, 61.05.cp, 63.20.dk

I. INTRODUCTION

Upon compression, bonding patterns established for molecular systems at ambient conditions change dramatically, causing profound effects on numerous physical and chemical properties and producing many new materials that cannot be formed at normal conditions.[1] Molecular hydrogen (H_2) is most fundamental, and the intramolecular H-H covalent bond is typically viewed as robust and a source of rich physics at its condensed state.[2] Recent experiments have unexpectedly revealed that H_2 molecules can interact with other full-shell molecules CH_4, SiH_4, H_2O, and NH_3BH_3, and even with inert gas Ar and Xe at readily accessible pressures with the formation of intriguing van der Waals compounds CH_4-H_2,[3] SiH_4-H_2,[4,5] H_2O-H_2,[6–8] NH_3BH_3-H_2,[9] Ar-H_2,[10] and Xe-H_2.[11] The fraction of hydrogen in these compounds is extremely high, e.g., 89% in $SiH_4(H_2)_2$ (Refs. 4 and 5) and even 94% in $Xe(H_2)_8$.[11] The advent of these compounds opens up an era of high-pressure chemistry on synthesis of hydrogen-rich materials, which could have potential application on hydrogen storage and even pursue high-temperature superconductors.[12]

Unfortunately, none of the crystal structures of the above H_2-containing compounds has been unambiguously solved so far, which are central and fundamental to address the hydrogen chemistry, important for a broad range of problems spanning fundamental chemistry, planetary, and materials science, and to the understanding of the efficiency of hydrogen storage and potential superconductivity. The experimental structure determination remains a major challenge since x-ray diffraction (XRD) data can only provide the structural information of heavier atoms. The theoretical structural determination of hydrogen in these compounds is thus strongly demanded and becomes feasible only with the recent fast development of crystal structure prediction techniques, e.g., genetic algorithm,[13–15] random structure searching,[16] metadynamics,[17,18] etc.

The two experimental studies on $SiH_4(H_2)_2$ (Refs. 4 and 5) have presented fine XRD and Raman data. This provides theory an excellent opportunity to determine the crystal structure of $SiH_4(H_2)_2$ and allows us to reveal the H_2 dynamics. Here, the theoretical exploration on the crystal structure of $SiH_4(H_2)_2$ has been performed by the genetic algorithm on crystal structure prediction.[13–15] We find that SiH_4 molecules form a tetragonal lattice with H_2 molecules occupying the interstitial sites. More intriguingly, through the frozen orientation technique, the unexpected orientationally disordered nature of H_2 molecules has been unambiguously determined, as supported by the excellent mutual agreement between theory and experiment on XRD pattern, Raman spectrum, and equation of states (EOS).[5]

II. COMPUTATIONAL METHODS AND DETAILS

Genetic algorithm[13–15] employed here was designed to search for the structures possessing the lowest energy at given P/T conditions. The details of the search algorithm and its several applications have been described elsewhere.[13,19–25] The underlying *ab initio* structure relaxations were performed using density-functional theory (DFT) within generalized gradient approximation (GGA),[26] as implement in the VASP code.[27] The all-electron projector-augmented wave method[28] was adopted for Si and H with valence electrons of $3s^23p^2$ and $1s^1$ and cutoff radii of 1.9 a.u. and 0.8 a.u., respectively. A plane-wave kinetic-energy cutoff of 1000 eV for all phases, and the use of Monkhorst-Pack k meshes of $8\times8\times8$ and $6\times6\times4$ for tI18 and oP18 structures, respectively, were shown to give excellent convergence of the total energy. In the geometrical optimization, all forces on atoms were converged to be less than 0.001 eV/Å, and the total stress tensor was reduced to the order of 0.01 GPa. Raman intensities are computed from the second-order derivative of the electronic density matrix with respect to a uniform electric field[29] through the QUANTUM-ESPRESSO package.[30] Norm-conserving scheme was used to generate the Perdew-Burke-Ernzerhof GGA density functional[26] pseudopotentials for Si and H. Particular care was paid to avoid any unnecessary errors caused by the use of two different codes. The same force convergence threshold (0.001 eV/Å) for structural optimizations was applied. We have computed the EOS and band structures of $SiH_4(H_2)_2$ by using the two codes of VASP and QUANTUM-ESPRESSO. Excel-

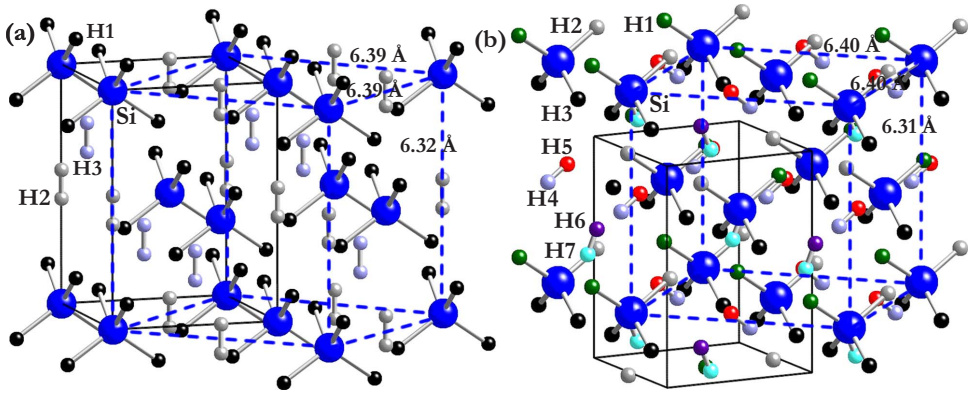

FIG. 1. (Color online) Crystal structures of $SiH_4(H_2)_2$: (a) tI18 and (b) oP18. The inequivalent Si (large sphere) and H (small sphere) atoms are labeled. Note that $(H2)_2$ molecule has a bond length of 0.748 Å, slight different with that (0.752 Å) of $(H3)_2$. The dashed lines in (a) and (b) denote the distorted fcc lattice of Si.

lent mutual agreements were evidenced, supporting the unbiased results by using different codes.

III. RESULTS AND DISCUSSION

Two types of evolutionary simulations were performed: (1) fixed-cell simulation with four $SiH_4(H_2)_2$ formula units (f.u.) per cell at the experimental lattice parameters (a =6.426 Å at 6.8 GPa)[5] and (2) variable-cell simulations at 6.8 and 10 GPa with 1–4 f.u./cell. Both fixed- and variable-cell simulations predict a body-centered tetragonal $I\bar{4}m2$ structure [2 f.u./cell, named as tI18, Fig. 1(a)]. Variable-cell simulations give another energetically competitive orthorhombic $Pmn2_1$ structure [2 f.u./cell, named as oP18, Fig. 1(b)]. Both tI18 and oP18 structures are constructed by weakly interacted SiH_4 and H_2 molecules, forming typical van der Waals molecular compounds. It is interesting to note that in the two structures SiH_4 molecules basically keep its original tetragonal packing with Si atoms sitting at a tetragonal sublattice [solid cell in Fig. 1(a)] and H_2 molecules occupy the interstitial sites of Si lattice. If we consider a larger cell (dashed cell in Fig. 1), where for tI18 at 6.8 GPa, $a=b=6.39$ Å approximately equals to $c=6.32$ Å, the Si lattice can thus be viewed as a slightly distorted face-centered-cubic (fcc) lattice. The same is also applied to oP18 with $a=b=6.40$ Å and $c=6.31$ Å at 6.8 GPa. This could naturally explain the experimental suggestion of a fcc structure.[5] It is remarkably that the simulated XRD patterns [Fig. 2(a)] for both tI18 and oP18 structures agree perfectly with the experiment data.[5] The lattice parameters of the tI18 and oP18 structures for $SiH_4(H_2)_2$ optimized at 6.8 GPa are listed in Table I. Phonon calculations performed for both structures at 6.8 GPa have demonstrated their structural stabilities in view of the absence of any imaginary frequencies.

The calculated EOSs for the tI18 and oP18 structures were compared with experiments[5] in Fig. 2(c). Excellent mutual agreement between theory and experiment gives another support for the validity of main (here SiH_4) framework of tI18 and oP18 lattices. However, it is surprisingly found that the two structures are energetically nearly degenerated in a large pressure range, i.e., enthalpy difference in the range of 6.8–35 GPa is less than 1 meV/f.u. We have then examined these two crystal structures and found out that the only dif-

TABLE I. Calculated lattice parameters of tI18 and oP18 structures for $SiH_4(H_2)_2$ at 6.8 GPa.

Space group	Lattice parameters (Å)	Atom	x	y	z
$I\bar{4}m2$ (tI18)	a=4.5187	Si(2a)	0	0	0
	b=6.3169	H1(8i)	0.2685	0	0.1345
		H2(4e)	0	0	0.4408
		H3(4f)	0	0.5	0.1905
$Pmn2_1$ (oP18)	a=4.5223	Si(2a)	0	0.7521	0.3586
	b=4.5223	H1(2a)	0	0.4842	0.4935
	c=6.3071	H2(2a)	0	0.0205	0.4931
		H3(4b)	0.2676	0.7532	0.2232
		H4(2a)	0	0.7063	0.8039
		H5(2a)	0	0.7823	0.9093
		H6(2a)	0	0.2341	0.1622
		H7(2a)	0	0.2961	0.0516

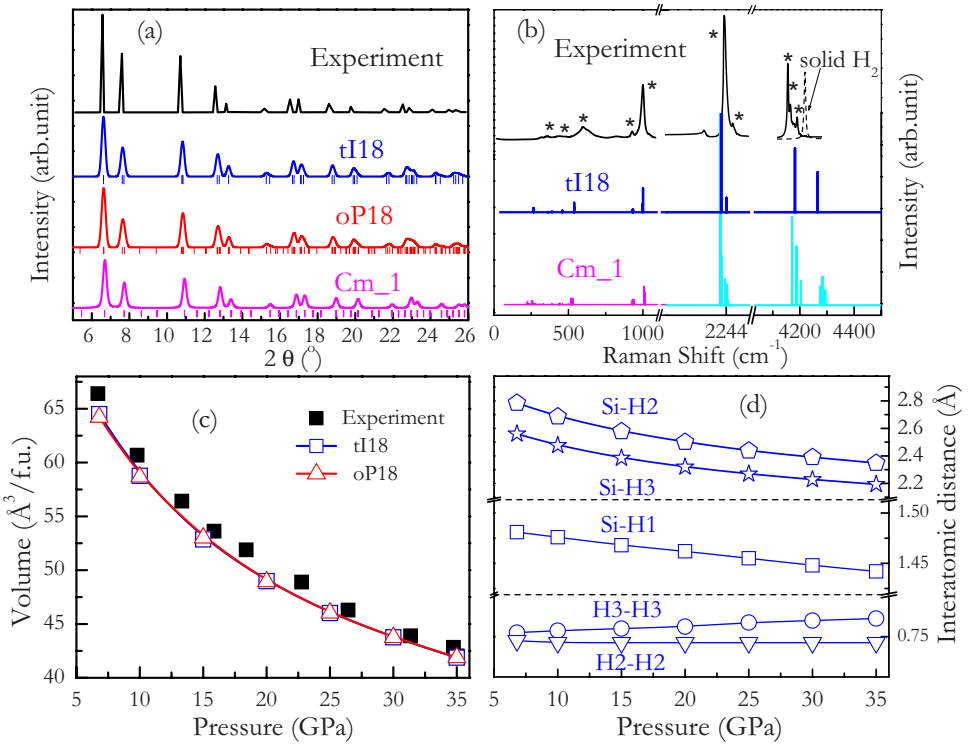

FIG. 2. (Color online) (a) The simulated XRD patterns and (b) Raman spectra for the tI18, oP18, and *Cm*_1 structures along with experimental data (Ref. 5). Vertical bars in (a) indicate the calculated positions of the diffraction lines and the asterisks in (b) represent the main Raman peaks in experiment (Ref. 5). (c) Theoretical EOS of tI18 and oP18 structures compared with experiment data (Ref. 5). (d) Pressure dependence of various interatomic distances in tI18 structure.

ference between the two structures is on the orientations of H_2. The removal of H_2 molecules from the two structures results in one structure. This motivated us a particularly designed total-energy calculation through frozen orientation technique, i.e., gradually rotating H_2 molecules in (100) and (110) planes [Figs. 3(a) and 3(b)] while remaining the center of H_2 unchanged. The obtained energy curves with variation in pressure are presented in Fig. 3(c) and it is found that the

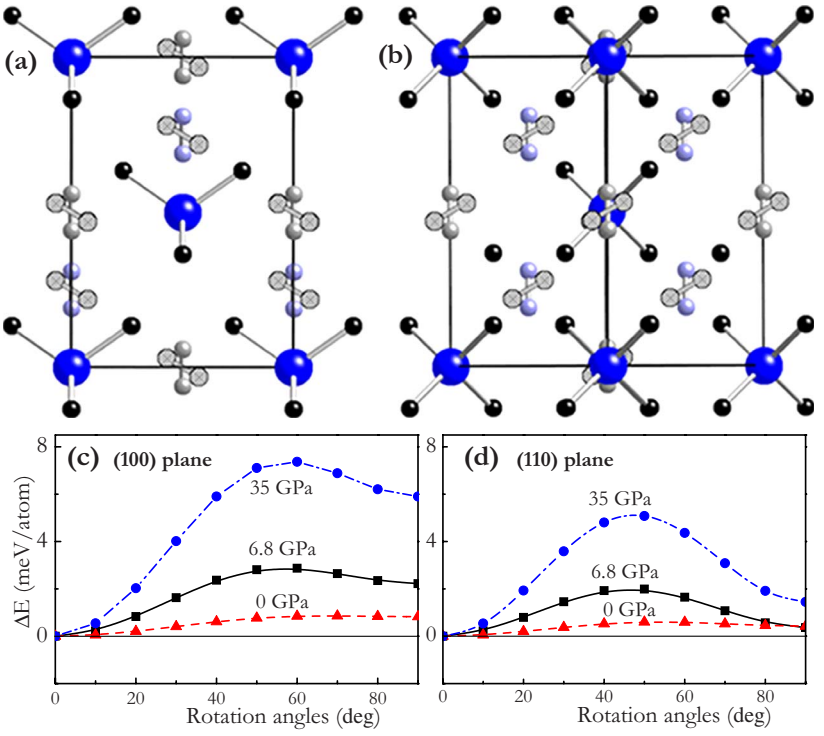

FIG. 3. (Color online) (a) and (b) are illustrations of H_2 rotations in (100) and (110) planes in the tI18 structure, respectively. (c) and (d) are total energies with the variation in H_2 orientations at 0 GPa, 6.8 GPa, and 35 GPa in (100) and (110) planes, respectively.

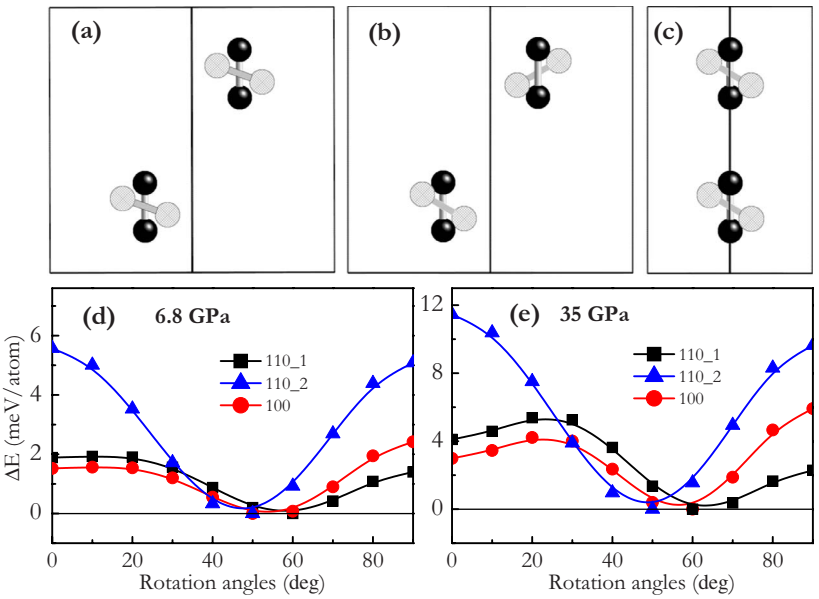

FIG. 4. (Color online) [(a) and (b)] The illustration of H_2 rotations in the (110) and (c) $(1\bar{1}0)$ planes of hcp-H_2. The black atoms represent the initial hydrogen molecules while the gray atoms are the rotated hydrogen molecules. (d) and (e) are the total energies of hcp-H_2 with H_2 rotations at 6.8 GPa and 35 GPa, respectively. The lowest energies are scaled as the zero energy.

maximal energy barriers of these H_2 rotations increase from ~1.0 to less than 8.0 meV/atom with pressure up to 35 GPa. Such low-energy barrier could naturally lead to a free rotator of H_2, resulting in an orientational disorder.

To support the above argument, we also performed the same rotational energy barrier calculations on the orientationally disordered hexagonal closed-packed (hcp) phase of solid H_2.[13] As shown in Fig. 4, the resulting maximal energy barrier in solid H_2 is actually larger (~12 meV/atom at 35 GPa). In fact, this is not unreasonable since the nearest-neighboring distance of SiH_4-H_2 in $SiH_4(H_2)_2$ is 2.304 Å at 6.8 GPa, evidently larger than that (1.952 Å) of nearest H_2-H_2 in hcp-H_2 at the same pressure. This allows relatively looser H_2 environment and lower energy barriers to make the H_2 orientational disorder possible in $SiH_4(H_2)_2$.

Since DFT_GGA calculation has certain degree of failure in dealing with the van der Waals interaction, we have employed a quantum chemical calculation based on the coupled cluster with single and double excitations technique (CCSD) (Ref. 31) known for reliable calculations of van der Waals interaction[32] to check the validity of the above DFT_GGA energy barrier. Figure 5 presents comparisons of DFT_GGA and CCSD energy barriers with variation in H_2 rotations for SiH_4-H_2 and H_2-H_2 interactions. Since the current CCSD calculation is not allowed for a crystal, we therefore designed specific clusterlike configurations to mimic the periodic crystal systems: (i) for evaluation of the SiH_4-H_2 interaction the configuration [inset of Fig. 5(a)] of one H_2 with four nearest surrounded SiH_4 molecules extracted from the tI18 structure of $SiH_4(H_2)_2$ was proposed while (ii) for H_2-H_2 interactions, 16 H_2 molecules in the $2\times2\times2$ supercell of hcp-H_2 was designed as seen in the inset of Fig. 5(b). Good mutual agreement between DFT_GGA and CCSD results has been amazedly found, indicating that our energy barrier results basing on DFT_GGA are quite reliable. This is not unexpected since although DFT_GGA has a failure in describing the absolute van der Waals energy, the systematic errors might be cancelled out in a large extent when seeking a relative energy.

Raman spectra are essential for identifying structures, especially important for hydrogen-containing compounds. Since the Raman spectra of tI18 and oP18 are quite similar, we therefore only present the result of tI18 to compare with experiments[5] as depicted in Fig. 2(b). The Raman spectrum is clearly divided into three groups where the two low-frequency groups are contributed by the vibrations of SiH_4 molecules and the highest energy region is from H_2 vibrons. Excellent agreement between theory and experiment is found

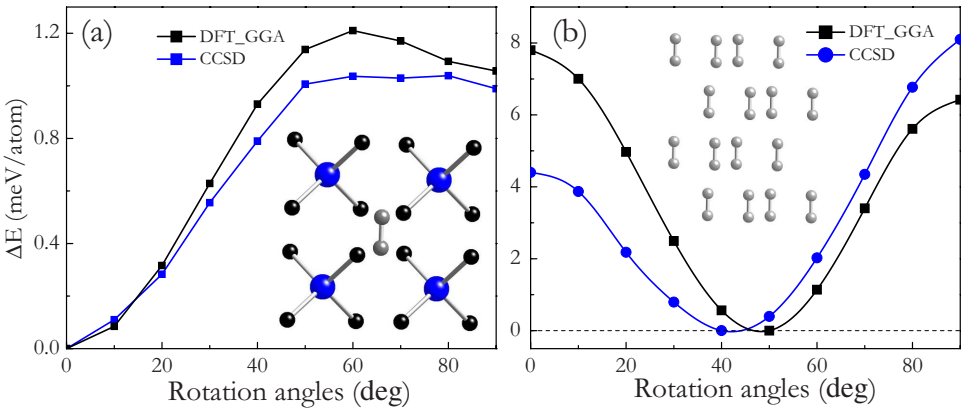

FIG. 5. (Color online) Comparisons of DFT_GGA and CCSD energy barriers with variation in H_2 rotations for (a) SiH_4-H_2 and (b) H_2-H_2 interactions.

in the two lower frequency groups. This together with the XRD evidence [Fig. 2(a)] have convinced us to announce a resolved sublattice occupied by SiH_4 molecules in $SiH_4(H_2)_2$. However, although the major experimental peak in high-frequency H_2 vibrons is reproduced, clear discrepancies are evidenced with the missing of several experimental shoulder peaks in theory. Group theory analysis revealed that two (four) H_2 molecules in the primitive cell of tI18 (oP18) structure leave only two (four) Raman vibron modes, which are quantitatively less than the experimental observation of at least seven vibrons.[5] This discrepancy is understandable if one considers the true fact that H_2 is orientationally disordered in $SiH_4(H_2)_2$. This disorder inevitably reduces the structural symmetry, leading to a larger number of inequivalent H_2 molecules and thus more Raman vibrons.

To validate this scenario, we have constructed appropriate supercells [dashed cells in Figs. 1(a) and 1(b)] for tI18 and oP18 structures, both containing four $SiH_4(H_2)_2$ units, to mimic all possible orientations of H_2. By randomly changing the H_2 orientations, we have captured many instant structures, but after fully structural optimization, many of them gradually transform back to either tI18 or oP18 structure. Only eight new structures, two *Cm*, two *P*222, two $P\bar{4}2m$, one *P*2, and one $P\bar{4}$ structures remain stable after the optimization. Note that the choice of these structures does not revise the SiH_4 sublattice, thus the simulated XRD and lower energy Raman spectra remain nearly invariant [Figs. 2(a) and 2(b)]. Nevertheless, these new structures contain eight H_2 molecules in the primitive cell with which all intramolecular H-H bond lengths are slightly different, leading to eight H_2 Raman vibrons. Indeed, we found that Raman vibrons of these structures can reproduce well the experimental data[5] as shown in Fig. 2(b), where only the result of *Cm*_1 is presented as an illustrative case. Note that experiment did not observe the highest frequency vibrons (above 4200 cm^{-1}),[5] which might be attributed to its overlap with the extremely strong Raman peak of pure solid H_2. It is noteworthy that the eight structures are all dynamically unstable by evidence of the significant imaginary phonon frequencies. This resembles with what was found in solid H_2, where the hcp phase with most of suggested H_2 orientations were dynamically unstable except for a few particular orientations.

The current study on $SiH_4(H_2)_2$ has notable implications on other such van der Waals compounds. The available lattice data for heavy atoms indexed from XRD measurement and the suggested positions of H_2 center in H_2O-H_2,[8] CH_4-H_2,[3] Ar-H_2,[10] and Xe-H_2 (Ref. 11) enable us to roughly estimate the nearest intermolecular distances, ~2.84 Å for H_2O-H_2 (3.1 GPa), ~2.80 Å for CH_4-H_2 (6.2 GPa), ~2.67 Å for Ar-H_2 (6.2 GPa), and 2.86 Å for Xe-H_2 (4.9 GPa). These values are evidently larger than that (2.304 Å) of $SiH_4(H_2)_2$, implying that orientational disorders of H_2 molecules in these compounds are highly possible.

Earlier experiments reported two distinct H_2-bond behaviors under pressure: (i) weakening in $SiH_4(H_2)_2$,[5] H_2O-H_2,[7] and Xe-H_2,[11] (ii) while hardening in CH_4-H_2,[3] NH_3BH_3-H_2,[9] and Ar-H_2.[10] To understand the intriguing weakening of H_2 bond observed in $SiH_4(H_2)_2$, the pressure dependence of the intramolecular and intermolecular bond distances in tI18 structure was plotted in Fig. 2(d). Two types of intramolecular H-H bonds with distances of 0.748 Å (H2-H2) and 0.752 Å (H3-H3) are found at 6.8 GPa and slightly longer than that (0.743 Å) in solid H_2. With increasing pressure, it is interesting to find that the H2-H2 bond keeps nearly constant while H3-H3 bond increases to 0.757 Å at 35 GPa, which is responsible for the observed softening of H_2 Raman vibrons.[5] It is noted that $(H3)_2$ molecule was trapped inside a tetragonal SiH_4 cage with a nearest Si-H3 distance of 2.56 Å while $(H2)_2$ stays in a relatively larger octahedral cage with a larger nearest Si-H2 length of 2.79 Å. The fairly weak interaction between SiH_4 and H2 results in an insensitive pressure response on H2-H2 bond. However, analysis of the orbital interactions via the crystal orbital Hamilton population[33] show that the one-particle bond energy[34] of Si-H3 decreases from −0.009 eV at 6.8 GPa to −0.036 eV at 35 GPa, indicating the slightly increased covalent interaction (though still weak) between Si and H3 under pressure, which is the main cause for the observed weakening of H3-H3 bond. The current results in $SiH_4(H_2)_2$ might shed light on the weakening of H_2 bond in H_2O-H_2 and Xe-H_2 compounds. However, the physical mechanism of H_2 bond hardening in CH_4-H_2, NH_3BH_3-H_2, and Ar-H_2 under pressure remains unknown and needs future exploration.

IV. CONCLUSION

In conclusion, first-principles calculations have been employed to explore the crystal structure of the synthesized $SiH_4(H_2)_2$ constructed by weakly interacted SiH_4 and H_2 molecules. SiH_4 molecules in $SiH_4(H_2)_2$ have been found to adopt a tetragonal (or distorted fcc) sublattice with the interstitial sites occupied by H_2 molecules. The available fine experimental XRD and Raman data allow us to reveal the orientationally disordered nature of H_2 molecules. The genetic algorithm for crystal structure prediction does not guarantee a must global minimum but the successful application on the determination of crystal structure of $SiH_4(H_2)_2$ has witnessed us again its great success. The current theoretical results provide important knowledge on novel H_2 physics for other high-pressure H_2-containing van der Waals systems, e.g., H_2O-H_2, CH_4-H_2, NH_3BH_3-H_2, Ar-H_2, and Xe-H_2.

ACKNOWLEDGMENTS

We are thankful for financial support from the National Natural Science Foundation of China under Grant No. 10874054 and the China 973 Program under Grant No. 2005CB724400. G.G. is also grateful to the Project No. 20092004 supported by Graduate Innovation Fund of Jilin University. We thank C. J. Tian for his help in the CCSD calculations and discussions.

*Author to whom correspondence should be addressed; mym@jlu.edu.cn

[1] R. J. Hemley, Annu. Rev. Phys. Chem. **51**, 763 (2000).
[2] I. F. Silvera, Rev. Mod. Phys. **52**, 393 (1980).
[3] M. S. Somayazulu, L. W. Finger, R. J. Hemley, and H. K. Mao, Science **271**, 1400 (1996).
[4] S. Wang, H. Mao, X. J. Chen, and W. L. Mao, Proc. Natl. Acad. Sci. U.S.A. **106**, 14763 (2009).
[5] T. A. Strobel, M. Somayazulu, and R. J. Hemley, Phys. Rev. Lett. **103**, 065701 (2009).
[6] W. L. Mao and H. Mao, Proc. Natl. Acad. Sci. U.S.A. **101**, 708 (2004).
[7] W. L. Mao, H. Mao, A. F. Goncharov, V. V. Struzhkin, Q. Guo, J. Hu, J. Shu, R. J. Hemley, M. Somayazulu, and Y. Zhao, Science **297**, 2247 (2002).
[8] W. L. Vos, L. W. Finger, R. J. Hemley, and H.-k. Mao, Phys. Rev. Lett. **71**, 3150 (1993).
[9] Y. Lin, W. L. Mao, and H. Mao, Proc. Natl. Acad. Sci. U.S.A. **106**, 8113 (2009).
[10] P. Loubeyre, R. Letoullec, and J. P. Pinceaux, Phys. Rev. Lett. **72**, 1360 (1994).
[11] M. Somayazulu, P. Dera, A. F. Goncharov, S. A. Gramsch, P. Liermann, W. Yang, Z. Liu, H. Mao, and R. J. Hemley, Nat. Chem. **2**, 50 (2010).
[12] N. W. Ashcroft, Phys. Rev. Lett. **92**, 187002 (2004).
[13] A. R. Oganov, C. W. Glass, and S. Ono, Earth Planet. Sci. Lett. **241**, 95 (2006).
[14] A. R. Oganov and C. W. Glass, J. Chem. Phys. **124**, 244704 (2006).
[15] C. W. Glass, A. R. Oganov, and N. Hansen, Comput. Phys. Commun. **175**, 713 (2006).
[16] C. J. Pickard and R. J. Needs, Phys. Rev. Lett. **97**, 045504 (2006).
[17] R. Martoňák, A. Laio, and M. Parrinello, Phys. Rev. Lett. **90**, 075503 (2003).
[18] R. Martoňák, A. Laio, M. Bernasconi, C. Ceriani, P. Raiteri, F. Zipoli, and M. Parrinello, Z. Kristallogr. **220**, 489 (2005).
[19] A. R. Oganov, J. Chen, C. Gatti, Y. Ma, Y. Ma, C. W. Glass, Z. Liu, T. Yu, O. O. Kurakevych, and V. L. Solozhenko, Nature (London) **457**, 863 (2009).
[20] Y. Ma, A. R. Oganov, Z. Li, Y. Xie, and J. Kotakoski, Phys. Rev. Lett. **102**, 065501 (2009).
[21] Y. Ma, M. Eremets, A. R. Oganov, Y. Xie, I. Trojan, S. Medvedev, A. O. Lyakhov, M. Valle, and V. Prakapenka, Nature (London) **458**, 182 (2009).
[22] Y. Li, H. Wang, Q. Li, Y. Ma, T. Cui, and G. Zou, Inorg. Chem. **48**, 9904 (2009).
[23] G. Gao, A. R. Oganov, A. Bergara, M. Martinez-Canales, T. Cui, T. Iitaka, Y. Ma, and G. Zou, Phys. Rev. Lett. **101**, 107002 (2008).
[24] Q. Li, Y. Ma, A. R. Oganov, H. Wang, H. Wang, Y. Xu, T. Cui, H. K. Mao, and G. Zou, Phys. Rev. Lett. **102**, 175506 (2009).
[25] G. Gao, A. R. Oganov, P. Li, Z. Li, H. Wang, T. Cui, Y. Ma, A. Bergara, A. O. Lyakhov, T. Iitaka, and G. Zou, Proc. Natl. Acad. Sci. U.S.A. **107**, 1317 (2010).
[26] J. P. Perdew, K. Burke, and M. Ernzerhof, Phys. Rev. Lett. **77**, 3865 (1996).
[27] G. Kresse and J. Furthmüller, Phys. Rev. B **54**, 11169 (1996).
[28] G. Kresse and D. Joubert, Phys. Rev. B **59**, 1758 (1999).
[29] M. Lazzeri and F. Mauri, Phys. Rev. Lett. **90**, 036401 (2003).
[30] S. Scandolo, P. Giannozzi, C. Cavazzoni, S. de Gironcoli, A. Pasquarello, and S. Baroni, Z. Kristallogr. **220**, 574 (2005).
[31] G. D. Purvis and R. J. Bartlett, J. Chem. Phys. **76**, 1910 (1982).
[32] P. Jankowski and B. Jeziorski, J. Chem. Phys. **111**, 1857 (1999).
[33] R. Dronskowski and P. E. Bloechl, J. Phys. Chem. **97**, 8617 (1993).
[34] One-particle bond energy is the integral of the crystal orbital Hamilton population energy, which gives access to the contribution of a chemical bond to the distribution of one-particle energy. The more negative value of the one-particle bond energy indicates a stronger bond.